

# REPORT DOCUMENTATION PAGE

Form Approved  
OMB No. 0704-0188

Public reporting burden for this collection of information is estimated to average 1 hour per response, including the time for reviewing instructions, searching data sources, gathering and maintaining the data needed, and completing and reviewing the collection of information. Send comments regarding this burden estimate or any other aspect of this collection of information, including suggestions for reducing this burden to Washington Headquarters Service, Directorate for Information Operations and Reports, 4215 Jefferson Davis Highway, Suite 1204, Arlington, VA 22202-4302, and to the Office of Management and Budget, Paperwork Reduction Project (0704-0188) Washington, DC 20503.

PLEASE DO NOT RETURN YOUR FORM TO THE ABOVE ADDRESS.

1. REPORT DATE (DD-MM-YYYY)		2. REPORT DATE 07-19-1999		3. DATES COVERED (From - To) 12-15-98 to 07-18-99 FINAL	
4. TITLE AND SUBTITLE  "Inductive Plasma Physical Vapor Deposition for Shape Memory Alloys"				5a. CONTRACT NUMBER CN00167-99-C-0013	
				5b. GRANT NUMBER	
				5c. PROGRAM ELEMENT NUMBER	
6. AUTHOR(S)  Daniel M. Dobkin Simon I. Selitser				5d. PROJECT NUMBER	
				5e. TASK NUMBER	
				5f. WORK UNIT NUMBER	
7. PERFORMING ORGANIZATION NAME(S) AND ADDRESS(ES)  TimeDomain CVD Inc. 470 Division St. Campbell, CA 95008				8. PERFORMING ORGANIZATION REPORT NUMBER  TIM0007	
9. SPONSORING/MONITORING AGENCY NAME(S) AND ADDRESS(ES)  Joseph Teter Code 6840 Naval Surface Warfare Center, Carderock Div. 9500 MacArthur Blvd West Bethesda, MD 20817-5700				10. SPONSOR/MONITOR'S ACRONYM(S)	
				11. SPONSORING/MONITORING AGENCY REPORT NUMBER	
12. DISTRIBUTION AVAILABILITY STATEMENT  Approved for public release, SBIR report, distribution unlimited					
13. SUPPLEMENTARY NOTES					
14. ABSTRACT  This work sought to use inductive thermal plasmas to deposit superelastic alloys from a wire source. It was found that unbiased sources could not be heated sufficiently at the tip to produce a measurable deposition rate. NiTi and Cu films were deposited at very low rates (on the order of 10 nm/min) using roughly 200 VDC applied to the wire relative to the substrate. Thermal modeling suggests that pulse biasing is necessary to achieve high deposition rates.					
15. SUBJECT TERMS  inductive thermal plasma deposition					
16. SECURITY CLASSIFICATION OF:			17. LIMITATION OF ABSTRACT	18. NUMBER OF PAGES  23	19a. NAME OF RESPONSIBLE PERSON Daniel M. Dobkin
a. REPORT unclassified	b. ABSTRACT unclassified	c. THIS PAGE unclassified			19b. TELEPHONE NUMBER (Include area code) 408-378-7896

# **Inductive Plasma Physical Vapor Deposition for Shape Memory Alloys: Final Report**

Daniel M. Dobkin and Simon I. Selitser  
July, 1999

## **Table of Contents:**

1] Overview .....	2
2] Equipment Design .....	3
3] Wire Source Testing .....	8
4] Thermal Model of Wire Source.....	12
5] Equivalent Circuit Model of Thermal Plasma.....	16
6] Discussion and Conclusions .....	21
References:.....	23

19990903 146

**DTIC QUALITY INSPECTED 4**

**TimeDomain CVD Inc.**



## 1] Overview

The objectives of this project were:

- 1] **Modify and adapt a commercial Inductively Coupled Plasma Torch for use in Superelastic SMA deposition.**
- 2] **Optimize the process parameters with respect to deposition rate and uniformity.**
- 3] **Characterize the morphology and microstructure of deposited Superelastic SMA film as a function of process parameters.**
- 4] **Compare the properties of the film and their microstructure to films produced by other processes like PVD and Plasma Spray.**

During this project we modified a commercial torch for use in deposition. However, the use of a wire source for deposition was found to be difficult: no configuration we tested gave measurable deposition from an unbiased wire. The difficulty essentially arises from the high thermal conductivity of the wire: it is not possible to isolate heating to the tip of the wire without melting the supporting structure, using any continuous source of heat such as exposure to the plasma. We were able to implement a bias arrangement and apply a DC voltage to the wire, leading to deposition at a very low rate (roughly 100 Å/minute). The resulting films were strongly oxidized, probably due to the low deposition rate. Deposition was inconsistent, and was probably the result of transient heating from arcing between the wire and the substrate.

Thermal modeling suggests that a 20 KW pulsed power supply operating at 1% duty cycle, 100 μsecond pulse length, would enable reasonable deposition rates to be obtained. We were not able to implement a pulsed bias supply within the scope of the current project. In consequence, we could not address objectives (2), (3) and (4).

Details of this work are provided below.



## 2] Equipment Design

A block diagram of the deposition system is shown in figure 2.1.

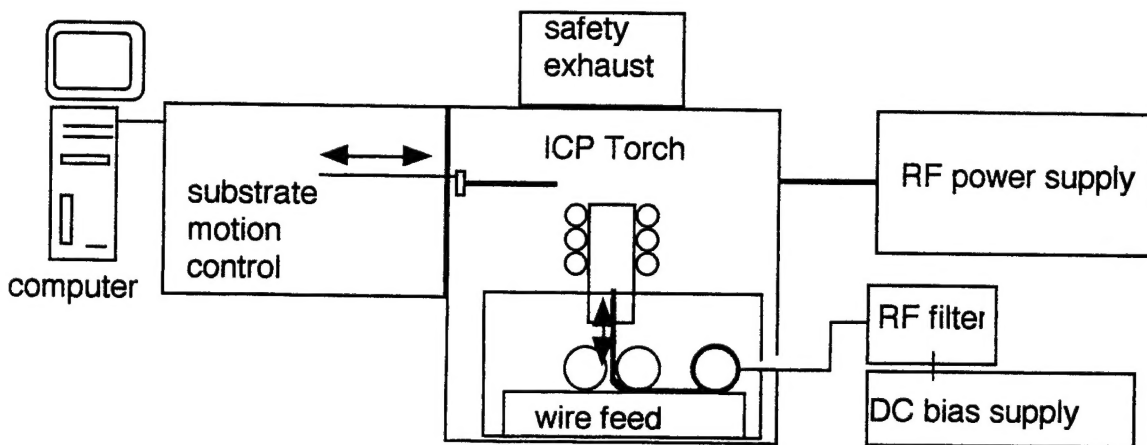


Figure 2.1: Block diagram of inductive thermal plasma deposition system.

### ***Torch and Power Supply***

The torch system is a modified commercial Perkin-Elmer 6500 ICP, originally intended for optical emission spectroscopy. The spectroscope and nebulizer have been removed. The access window for spectroscopy is used to insert the substrate motion wand. A custom Perkin-Elmer 27 MHz, 1800 W RF power supply is used. This supply allows for automatic cutoff of RF power on violation of any of the system interlocks or when excessive reflected power is detected, avoiding dangerous operating conditions and preventing damage to the power supply. Gas flow control employs conventional rotameters. Manual control is provided from the system front panel; there is no automated control. The system is about 15 years old.

Typical operating conditions for this system are:

- 15 slpm argon sheath gas
- 1-3 slpm argon center (plasma) gas
- 600 W power for ignition; thereafter 600-1800 W

We used the standard torch received with the commercial system for some experiments. This torch is composed of fabricated quartz containing the gas supply holes, inner and outer tubes in



a single piece, mounted onto what appears to be a machined phenolic base. The overall exit diameter is about 25 mm.

We also designed our own torch mount system, which mounts two concentric quartz tubes for plasma and sheath gases, simplifying torch modification and replacement.

A photograph of the modified system is shown in figure 2.2.



Figure 2.2: Modified Commercial ICP Torch System

### ***Substrate Motion System***

Substrate motion employed an Arrick Robotics MD-2 motion system controlled by a desktop computer. The system provides two axes of motion, and is capable of 0.125 mm positional resolution and speeds up to 20 cm/second. We typically used one-axis motion to carry the substrates over the torch one or more times, using travel speeds of 2-5 cm/second.

We constructed a simple mount to provide leveling and height adjustment. The completed system is shown in figure 2.3. Note that the sample holder is mounted at the end of long ceramic rod. We found that coupling of high-frequency excitation from the plasma into a metallic rod would interfere with smooth operation of the stepper motors when the substrate paddle was close to or in contact with the plasma; this phenomenon is discussed in more detail in section (5) below.



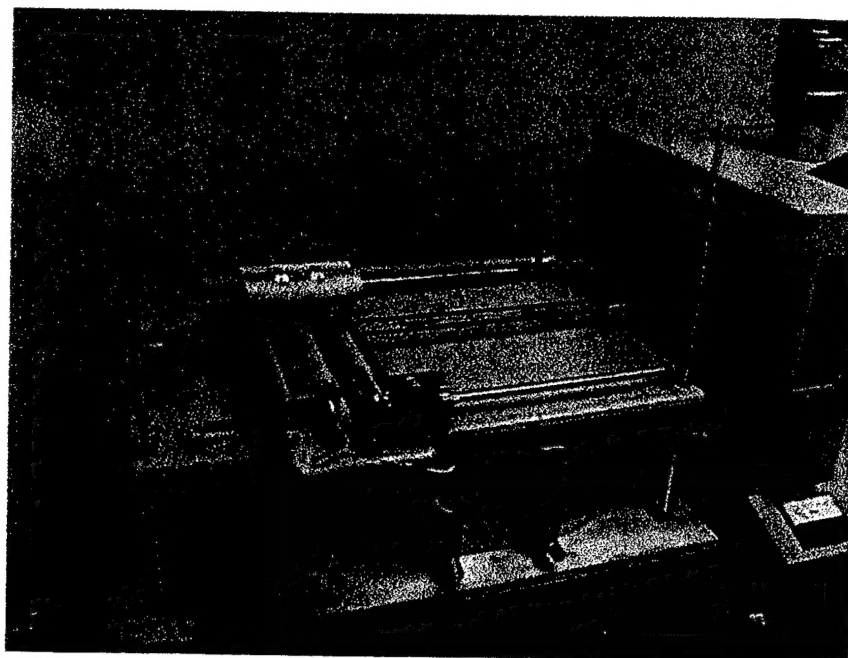


Figure 2.3: Substrate motion system

### ***Wire Source Design and Construction***

Wire is inserted into the plasma through a ceramic tube mounted in the center of the torch, with the exit of the ceramic tube roughly at the same height as the upper edge of the sheath flow (inner) quartz tube. The height can be adjusted a few mm in either direction. The wire feeding action is achieved by passing the wire between two plastic rollers from a spool. The rollers are driven by a gear and handle, so that the rate of feed of the wire can be adjusted in real time based on visual observation of the wire tip position and configuration. A photograph of the arrangement is shown in figure 2.4.



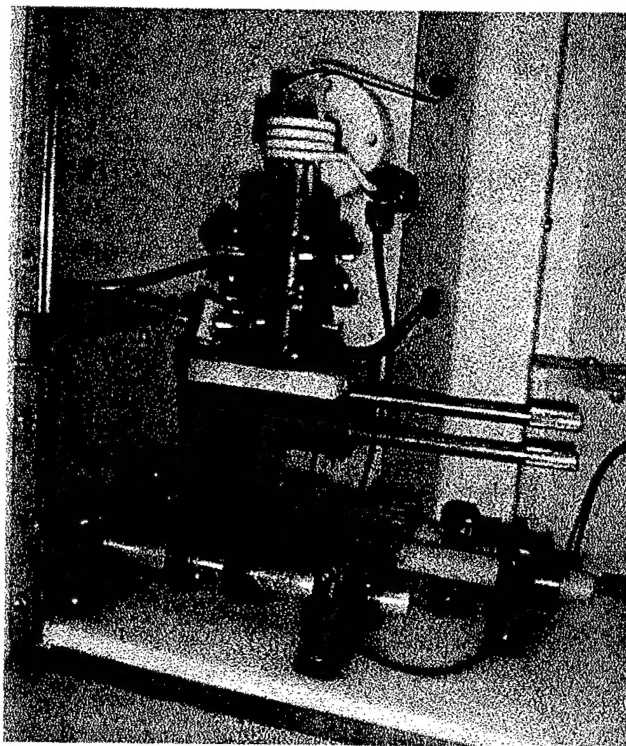


Figure 2.4: Wire feed apparatus positioned below torch

### ***Wire Biasing Provisions***

To apply bias to the wire source, the supply spool can be connected to a conventional copper feed wire, which after passing out of the torch enclosure is connected through a switch to a coaxial cable. We constructed a low-pass filter to minimize exposure of the DC power supply to 27 MHz coupled into the deposition source wire. The filter consisted of two hand-wound inductors of about  $1\ \mu\text{H}$  each in a tee configuration with a grounded 50 nFd capacitor between them. A schematic diagram is shown in figure 2.5.



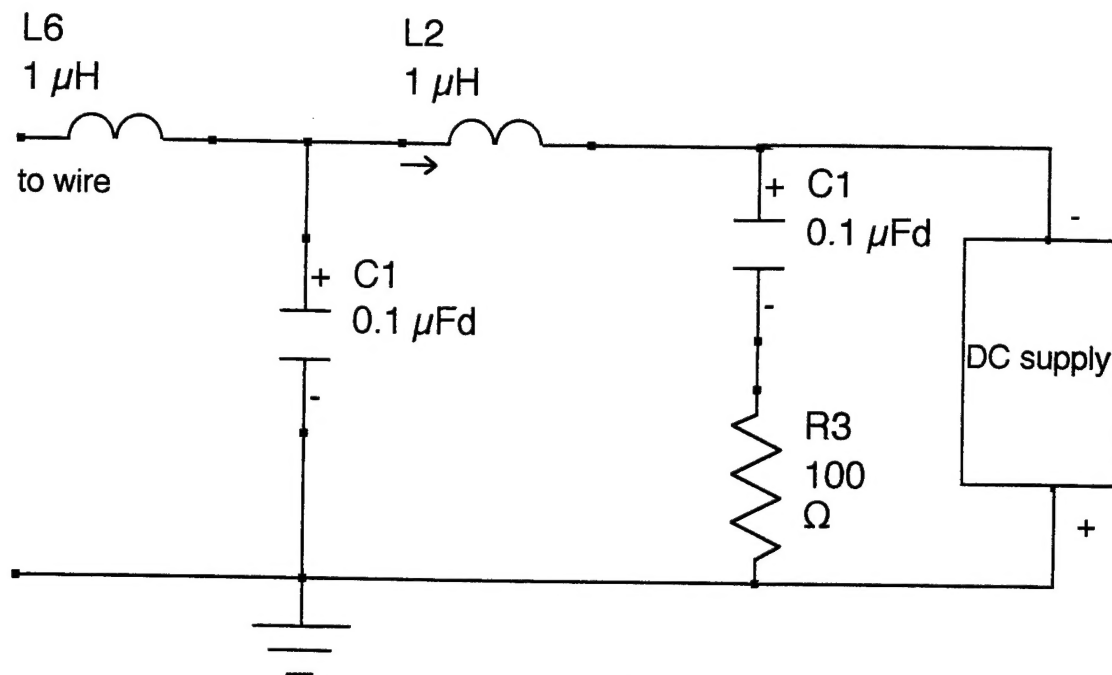


Figure 2.5: Low pass filter schematic

In order to obtain good common-mode rejection on this filter, we found it to be critical to construct the filter over a ground plane created by an aluminum plate, and to ensure low-inductance connections to all nominally grounded points in the circuit, as well as the power supply ground.

The bias is supplied by a Sorenson DCR 300-1.5B regulated DC power supply, which allows both voltage- and current-limiting operation up to 400 volts and 2 amperes. A photograph is shown as figure 2.6.





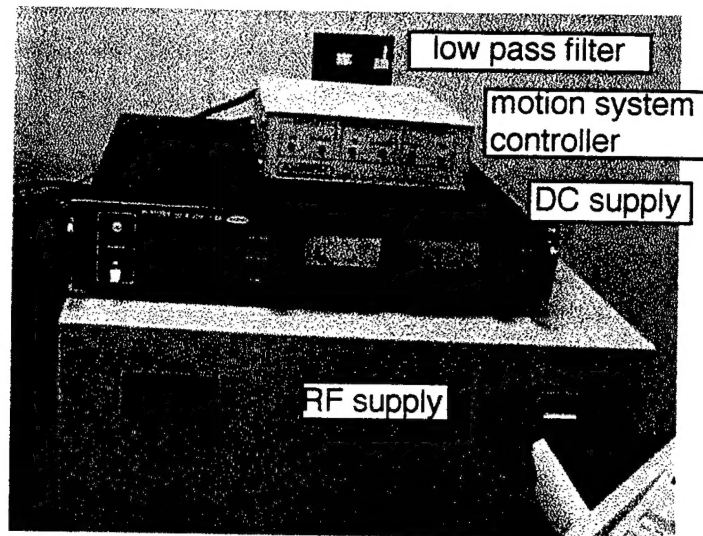


Figure 2.6: Low pass filter and DC bias supply, motion system controller, and RF power supply.

### 3] Wire Source Testing

Initial testing of wire source deposition was conducted without bias, using copper wire for cost reasons. After plasma ignition with the tip of the wire positioned 3-5 cm below the plasma within the ceramic tube, the wire was inserted into the tube until the wire tip became visible. Typical plasma conditions were as described in section (2) above, with RF power of 600-800 W.

We found that as the wire was raised towards the very hot plasma core, the tip of the wire would melt and form a roughly spherical ball, which would then descend down the wire until it sat roughly on the end of the ceramic tube. Thereafter slow continuous feeding of the wire would cause the molten ball to expand; balls as large as 3 mm in diameter were obtained from a wire of slightly less than 1 mm diameter by inserting about 10 cm of wire. (Slow continuous feeding of the wire was necessary at all times to avoid it becoming "stuck" in the ceramic tube; we found it necessary to immediately raise the tip of the wire a few cm after turning the plasma off to avoid the cooling ball becoming stuck to the ceramic tube.) We also noted that the ball was in some cases clearly rotating, presumably due to residual torque from induced currents. A photograph of such a ball under the plasma is shown in figure 3.1.



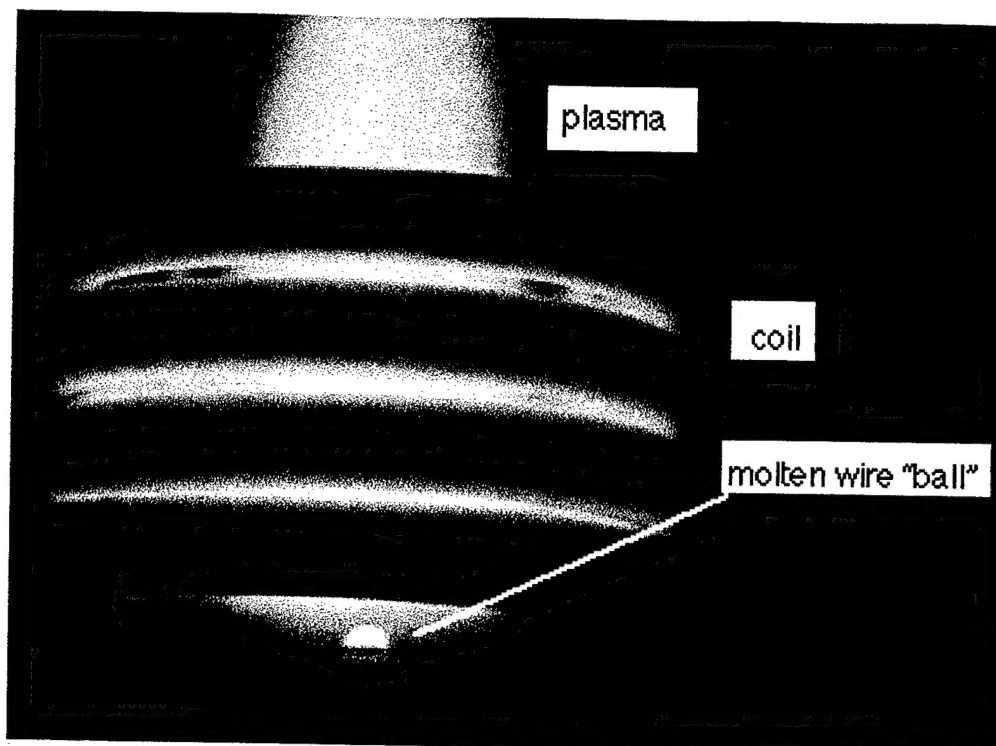


Figure 3.1: Wire inserted in plasma without bias

Similar results were obtained when the source wire was inserted (manually) in a horizontal orientation along a radius just above the upper edge of the torch confinement tube.

We attempted to deposit films from the heated wire ends by passing a substrate over the torch at varying heights from 1 to 3 cm, while feeding wire into the molten region. However, no detectable deposition occurred from either Cu or NiTi source wire under these conditions. The difficulty is undoubtedly due to the fact that conduction of heat along the wire is rapid, so that it is not possible to heat the surface of the wire to the very high temperatures required for rapid vaporization without melting the supporting wire and causing the ball to drop, reducing the heat flux and cooling the surface. This issue is discussed in more detail in section (4) below.

We then tried applying a negative bias to the wire using a power supply and low-pass filter as discussed above, in order to create localized heating and possibly also ion bombardment effects at the surface. As noted above and discussed in more detail in section (5) below, considerable RF coupling occurs between the exciting coil, the plasma, and the wire source, and thus precautions are needed to ensure that the DC power supply is isolated from this high frequency signal.



We explored bias levels from 30 to 250 V, with current flow up to 1 A, using both copper and NiTi wires. In all cases, the substrate was polished aluminum, with a shadow mask made of a slice of silicon to delineate deposition, and grounded in order to provide a current return path.

We found that application of bias gives rise to several interesting phenomena:

- intermittent arcs were found to occur between the plasma and the grounded substrate, as evidenced by easily audible “snapping” sounds and occasionally by erosion pits on the substrate, in addition to visual observations.
- the region near the wire was observed to glow more intensely with bias than without, but no arcing or localized filamentary plasma phenomena were visible around the wire tip (see figure 3.2).
- enhanced vaporization occurred, as evidenced by visible deposition on the substrates as well as a change in the color of the plasma

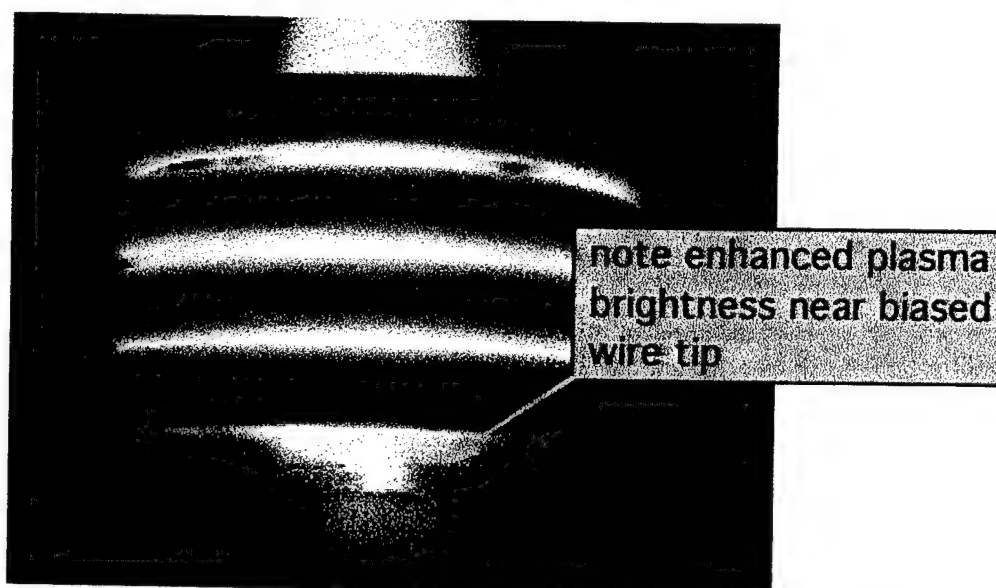


Figure 3.2: Photograph of wire tip in plasma with bias applied

Two samples each receiving about 30 seconds of deposition under the following conditions were analyzed by Auger at Charles Evans and Associates approximately one week after deposition: bias voltage 200 V, RF power 1000 W, with standard argon flows. A differentiated Auger spectrum of the as-deposited surface of the silicon sample is shown in figure 3.3. We see that the surface is predominantly Ni, Ti, and O, with traces of Al and a weak signal from the underlying Si substrate, and some C from the ambient. Thus, a NiTi film was deposited; it is heavily oxidized, though it is not possible to ascertain whether the oxidation took place during deposition or in subsequent ambient exposure.



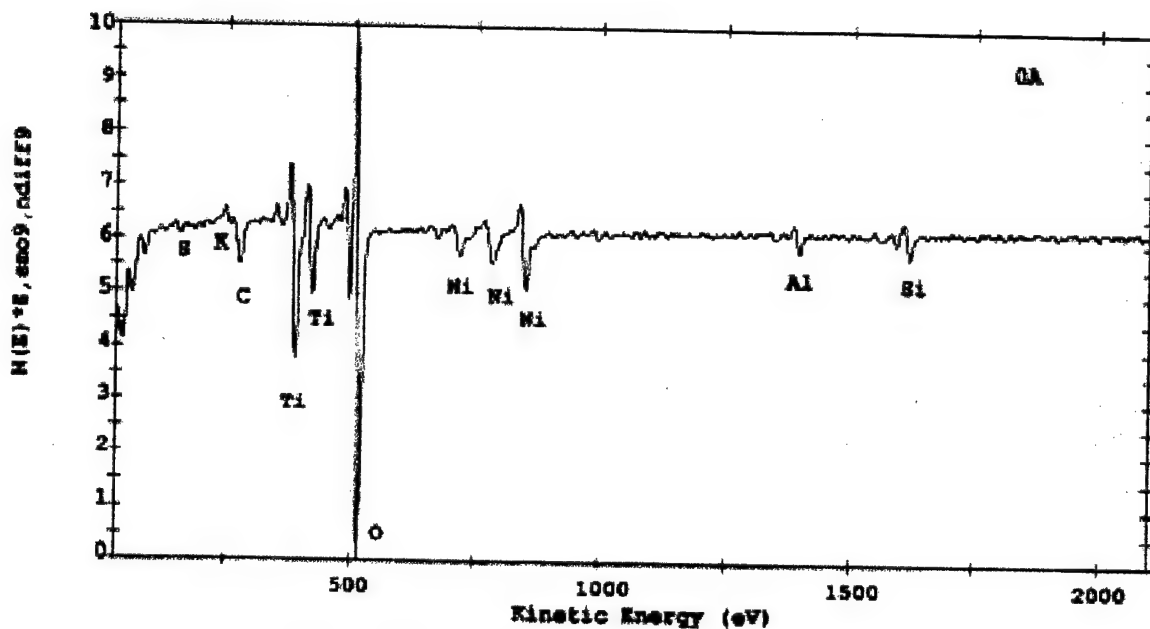


Figure 3.3: Silicon sample with NiTi film; as deposited

In table 3.1 we summarize estimated composition of the surface, after removal of about 20 Å by argon sputtering to eliminate adventitious carbon and other contaminants.

Table 3.1: Composition of film on silicon substrate, 20 Å removed

<u>element</u>	<u>concentration (at%)</u>
O	55.3
Ti	7.2
Ni	11.3
Al	7.5
Si	18.7

In figure 3.4 we show a profile of concentration vs. depth of several elements for this sample, constructed from spectra taken after removal of 0, 20 Å, 100 Å, and 150 Å by argon sputtering. We can assert that the film is about 70-80 Å thick, if we treat the interface as occurring when the change in concentration is 50% of the surface concentration.



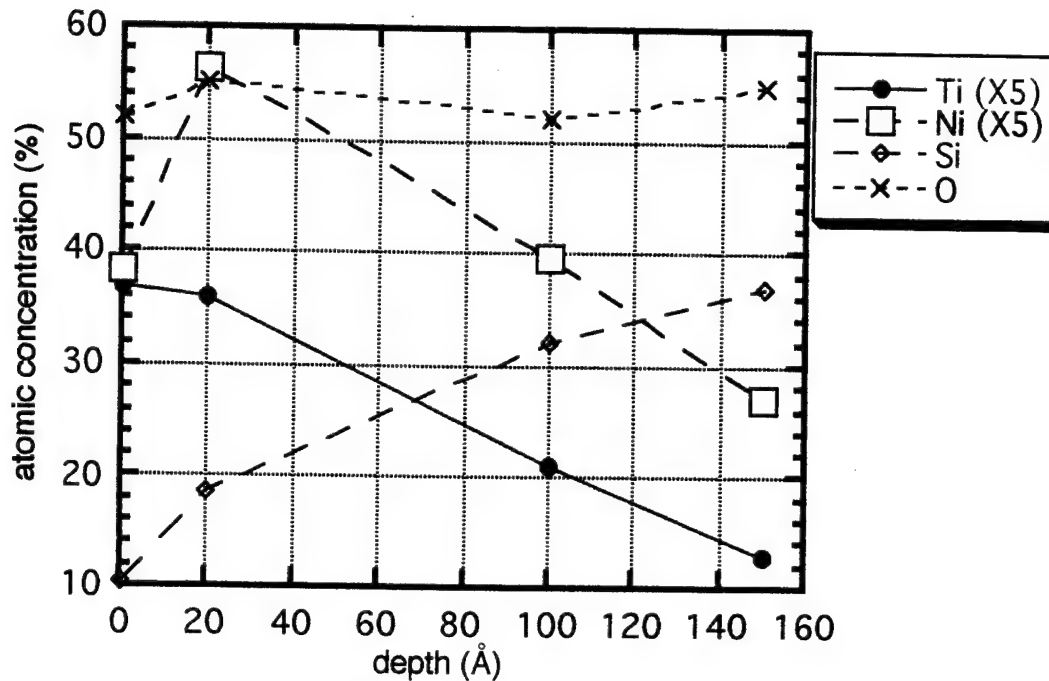


Figure 3.4: Auger depth profile for deposited NiTi film

#### 4] Thermal Model of Wire Source

To understand our results, let us consider heat transport to and within the wire. A simplified schematic of the electrically floating wire is shown in figure 4.1. We consider a cylindrical wire of radius  $R_w$  centered within the (ceramic) source cylinder of radius  $R_c$ , capped by a molten region of radius  $R_b$ . We approximate the rather complex gas flow configuration around the wire source by assuming there is a nearly stagnant region above the source, of extent roughly equal to the source radius:  $R_{st}$ .



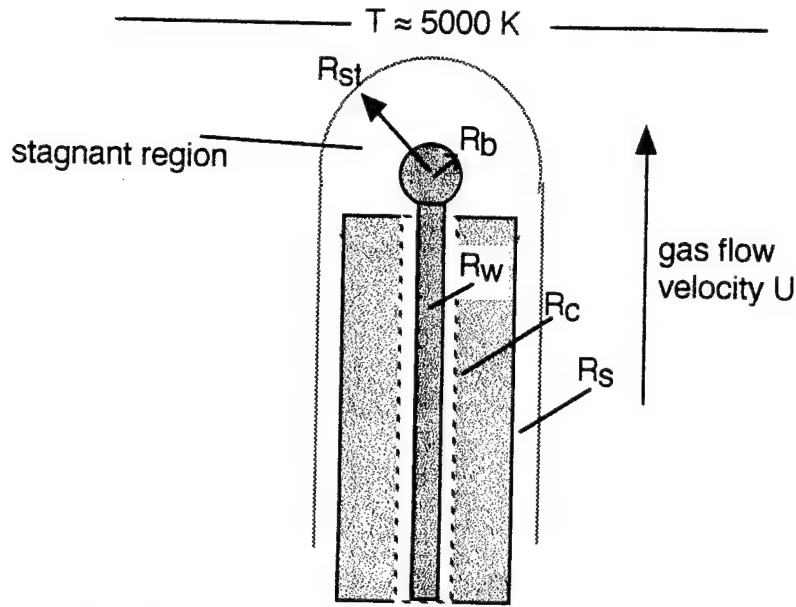


Figure 4.1: Simplified model for heat transport in the vicinity of the wire tip

To check whether this is reasonable, we estimate the Reynolds number of the tip-region flow:

tube area	2.5 cm <sup>2</sup>
flow	2.5 slpm
velocity*	60 cm/sec
$R_s$	0.6 cm
$v$	1
Re	36

For Reynolds numbers of this order, we expect flows which are irreversible (i.e. not “creeping” flow) but free of recirculation or turbulence. Thus a simple stagnation region model is acceptable for first-order estimates.

We will assume for simplicity that the edge of the stagnation region is at a uniform temperature of 5000 K, and that the spherical tip of the wire is essentially isothermal at some temperature  $T_b$ . In steady state the heat diffusion equation in the stagnant region becomes simply  $\nabla^2 T = 0$ , with solutions like  $1/r$  for a spherically symmetric region. The solution for the temperature in the upper hemispherical region is then roughly

$$T = \frac{R_b R_{st}}{R_{st} - R_b} \left[ \left( \frac{T_{st}}{R_b} - \frac{T_b}{R_{st}} \right) + \frac{T_b - T_{st}}{r} \right] \quad \{1\}$$



with heat flux at the tip equal to  $-K_{th} dT/dr$  evaluated at  $r=R_b$ :

$$K_{th} \left( -\frac{\partial}{\partial r} T \right) = K_{th} \left( \frac{R_{st}}{R_{st} - R_b} \right) \frac{T_b - T_{st}}{R_b} \quad \{2\}$$

(Here we have accounted only for conducted heat. The radiative heat transfer is certainly not negligible, but will depend strongly on the exact geometry and temperature of the plasma, and on the emissivity of the melt surface. Thus we should regard our estimates as a lower bound on heat transfer.)

Accounting for the fact that the wire is fed at a roughly constant speed  $V_w$ , the steady-state solution for the temperature along the wire is approximately:

$$T_{wire} = (T_b - T_{feed}) \exp \left( \frac{z V_w}{D} \right) + T_{feed} \quad \{3\}$$

where  $D$  is the thermal diffusivity in the wire,  $T_{feed}$  is the temperature of the wire entering the wire feeder (ignoring heating from the ceramic tube) and  $z$  is taken as 0 at the wire tip, decreasing (taking negative values) towards the feed. Typical values of  $D$  are about  $1 \text{ cm}^2/\text{sec}$  for Cu and 0.1 to 0.2 for Ni and Ti [1]. For a feed velocity of 0.1 cm/sec, the characteristic length for copper wire is about 10 cm, and for NiTi wire roughly 1.5 cm. These lengths are much longer than the diameter of the wire ( $< 1 \text{ mm}$ ), justifying the 1D approach. The diffusion length  $\sqrt{(4Dt)}$  for a typical experiment time of 25 seconds is about 10 cm in the case of copper, and 3 to 5 cm for NiTi, showing that the steady-state approximation is reasonable for both cases.

Let's consider some typical values of these quantities, specializing for the moment to copper. The total heat delivered to a 1 mm ball at the melting point of copper,  $1083^\circ\text{C}$  (1356 K), assuming a stagnation radius of 6 mm and heat delivery only to the top hemisphere, is roughly  $0.07 \text{ cm}^2 * 35 \text{ Watts/cm}^2$ , or about 2.2 watts. The heat required to melt the ball (i.e. the heat of fusion) is 7.6 Joules, so melting should take about 3.5 seconds. During this time, the diffusion length down the wire is around 3.7 cm, so from the point of view of the 1 mm wire a steady-state condition exists.

To achieve a reasonable deposition rate of e.g.  $10,000 \text{ \AA}/\text{min}$  at the substrate surface we need a vapor pressure of roughly 0.01 Torr, requiring the wire surface to be at a temperature of roughly 1500 K [2]. If we use this as the boundary condition for equation {3} above, we find that the temperature of the wire would exceed the melting temperature for a distance of roughly 1.3 cm: that is, we can't make the ball hot enough to evaporate rapidly and still keep the wire solid enough to support the ball, at least for reasonable feed rates at steady state. Since the heating



times are on the order of 1-2 seconds as noted above, the time required to heat the ball up is enough to melt the wire supporting the ball.

The general conclusions of this model are in accordance with our observations: if we increase the feed rate we can briefly elevate the molten ball into the plasma 2-3 mm, but within about 1 second the supporting wire melts again and the ball drops back onto the ceramic rod. Very high wire feed rates are required to localize the heat in a region less than 1 mm in extent, and the heat flux available is not sufficient to raise the temperature of the surface for rapid evaporation in the times allowed under those circumstances.

We therefore conclude that in order to fully exploit a wire feed for high-rate deposition, it is necessary to have a means of delivering large heat fluxes to the surface of the wire in very short times ( $\ll 1$  second). In view of this result, we suspect that the deposition we achieved using DC bias application may be due to brief transient heating accompanying the plasma-substrate arcs described in section (3) above.

To achieve controllable deposition, a pulsed bias capability would be required. In this case, most of the applied power would be deposited on the ball surface due to ion bombardment, as indicated schematically in figure 4.2. From the results of the calculations above, we find that a  $200\text{ }\mu\text{m}$  thick surface layer of the molten ball could be heated to 1800 K (for 1 Torr vapor pressure, 100 X higher than before to account for the lowered duty cycle) by the application of a  $100\text{ }\mu\text{sec}$  pulse with about 2 Joules total energy, assuming a 1% duty cycle. The peak power of the pulse is thus about 20 KW, and average power 200 W. The requirements for NiTi are similar to those encountered for Cu. The construction and integration of such a pulsed power system was judged beyond the scope of what could be accomplished in our current project.

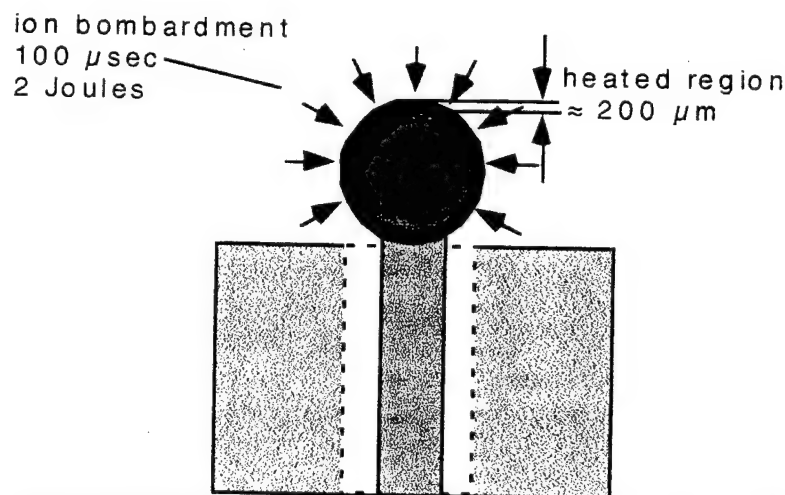


Figure 4.2: Use of pulsed bias allows delivery of heat to the surface of the molten ball; for short times, the heat will be limited to the surface layer while the average temperature remains low.





## 5] Equivalent Circuit Model of Thermal Plasma

The plasma is created by an inductive coil. The coil is sheathed in insulation, so there is no DC coupling to the plasma; thus the average plasma potential should be essentially zero. However, the plasma has a significant capacitive coupling to the coil, giving rise to large RF swings in the plasma potential, which would be expected to be effectively coupled to a conductive object inserted in or near the plasma.

To study this issue semi-quantitatively, we created a plausible equivalent circuit for the power supply / coil / plasma system, shown in figure 5.1.

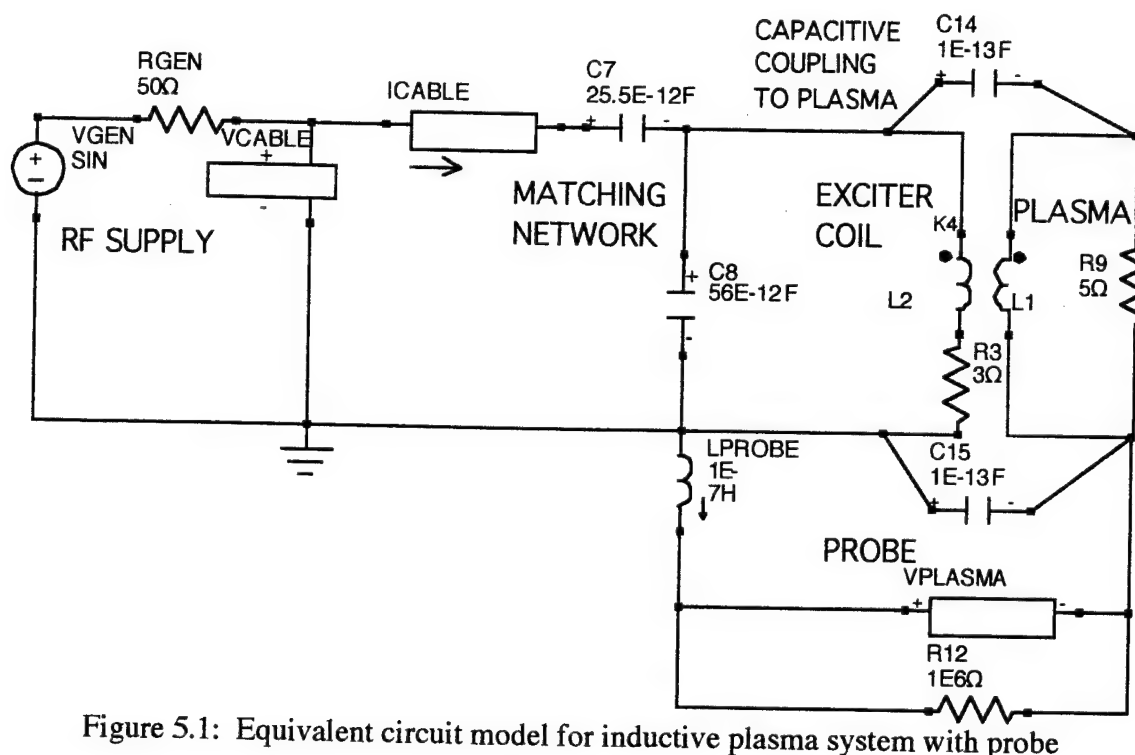


Figure 5.1: Equivalent circuit model for inductive plasma system with probe

The generator is modeled as an ideal generator with an internal resistance of 50 ohms. The matching network is modeled as two ideal capacitors, whose values can be varied to obtain a good match. The matching criteria are that  $V_{\text{cable}}$  is equal to  $1/2(V_{\text{generator}})$ , and both  $V_{\text{cable}}$  and  $I_{\text{cable}}$  are pure real with phase  $\approx 0$ . When these criteria are satisfied, the remainder of the circuit is acting as a second 50 ohm resistor from the generator output plane, and optimal power transfer is achieved.



The coil and plasma are modeled as an ideal transformer, with a coupling coefficient of about 0.3 (i.e. 3 turns on the primary, and a single turn on the secondary, which represents the plasma itself). A small resistance value associated with system losses is assigned to the primary side, and a somewhat larger value representing the actual power delivered to the plasma is assigned to the secondary. Capacitors C14 and C15 model the capacitive coupling from the coil to the plasma, through the air, quartz dielectric, and plasma sheaths. Two capacitors are used to balance coupling, since all parts of the coil should couple equally. The probe or wire is then modeled as sampling the plasma load, with an associated resistance and some inductance to ground. Simulations were performed using the commercially available program B<sup>2</sup> SPICE.

Matching behavior for this circuit is shown in table 5.1 and figure 5.2. We can see that the phase of the voltage across the system (the "cable" voltage) passes through 0 at around 28 MHz, showing that the load "looks" like a resistor: that is, it is matched to the resistive generator.

Table 5.1: Magnitude and phase of load currents and voltage vs. frequency

frequency (MHz)	mag(Vcable)/Vgen	phase(Vcable)	phase(Icable)
25.1	0.89	-19.4	62.3
27.1	0.75	-25.1	45.3
29.3	0.49	-0.6	0.5
31.6	0.85	10.0	-41.5
34.1	0.95	1.8	-31.6



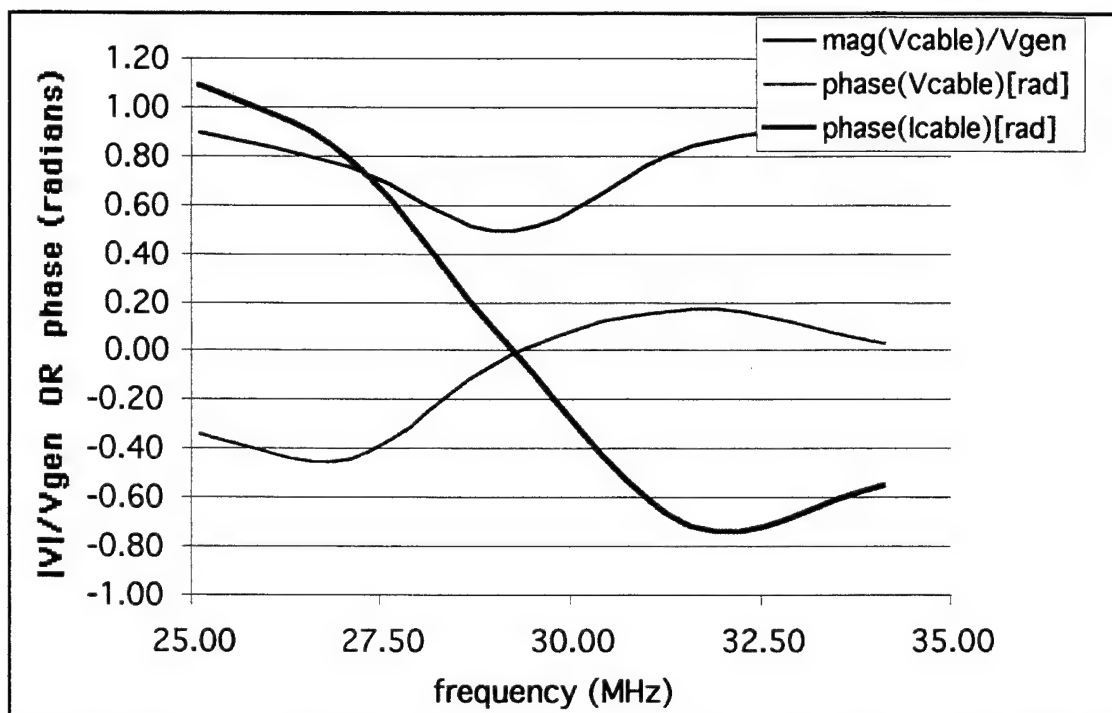


Figure 5.2: Magnitude of  $V_{\text{cable}}/V_{\text{gen}}$ , and phase of  $V_{\text{cable}}$  and  $I_{\text{cable}}$  (in radians), vs. frequency; note matched condition occurs at about 29.25 MHz.

Using this circuit, we can study the voltage coupled into the plasma through the capacitors can be significant. In figure 5.3 we show the plasma potential measured by a probe as a function of the probe resistance, for two different values of the coupling capacitors. Note that the data is obtained at the matched frequency, and the generator voltage has been set to 600 volts (peak), which will result in about 1300 Watts being delivered to the system.



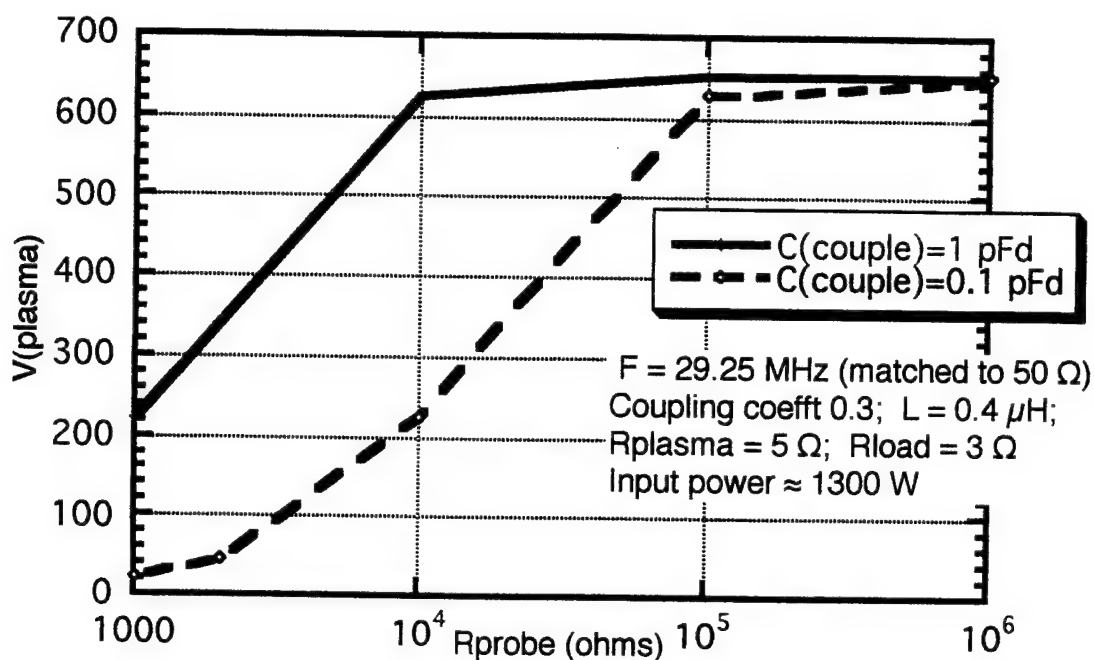


Figure 5.3: Effect of probe resistance and coupling capacitance on the plasma voltage measured by a probe

The actual values of coupling capacitance are difficult to estimate due to the complex geometry of the coil-torch-plasma system. A reasonable range can be asserted from the parallel-plate capacitance of an equivalent system consisting of the coil (about 2.3 cm diameter but with the wire actually filling about 2/3 of the area, 2 cm high) separated from the plasma by about 5 mm of air / sheath (the torch wall, with a dielectric constant of about 4, will contribute little to determining the capacitance):

$$A = (\pi)(2.3 \times 2)(2/3) \approx 10 \text{ cm}^2$$

$$C = \epsilon A/d = (8.86 \times 10^{-14}) (10/0.5) \approx 1.8 \text{ pFd}$$

which should roughly correspond to the sum of C14 and C15.

Thus it seems plausible to expect the plasma to exhibit a large voltage when floating, which can capacitively couple to nearby conducting objects or to conducting objects inserted in the plasma. The "internal impedance" of the plasma should be on the order of 10 to 100 KΩ; thus, a highly resistive probe would measure a large voltage, but very little RF current could be extracted. Naturally, no DC current is possible to extract unless a ground electrode, in reasonable contact with the plasma, is present.



These model results are quite consistent with our experimental observations:

- the large RF voltages can couple to objects near the plasma, explaining the necessity of insulating support for the sample holder to avoid interference with the motion system stepper motors.
- a grounded wire source does not experience significant RF current flow or RF heating vs. an electrically floating wire, since the low-impedance path to ground basically "shorts out" the plasma and pulls it to ground potential.

Table 5.2 summarizes results of measurements of voltages coupled through a 10X probe, with impedance about  $10\text{ M}\Omega$ , to a wire in the center of the plasma.

Table 5.2: Measured RF voltage on aluminum wire for various conditions; "b" is the height of the wire tip relative to the ceramic tube, in cm.

<u>condition</u>	<u>b</u>	<u>V(pk-pk)</u>
RF on, no plasma, 700 Watts	0	150
plasma on, 700 W	0	500
repeat , RF on, no plasma	-2	20
RF on, no plasma	2	20
RF on, no plasma	10	40
plasma on	10	500 [wire melted]
new wire tip, RF on, no plasma	0	140
new wire tip, plasma on	0	500, then < 100 in about 2 seconds
repeat after above, RF on, no plasma	0	20
plasma on	0	40

We also measured coupling to an aluminum plate placed in proximity to the generator, as shown schematically in figure 5.4. Again, as shown in table 5.3, large RF voltages were measured. Here we find that coupling is actually larger before the plasma is struck. This is presumably the consequence of higher Q and higher peak voltage in the absence of the losses associated with the plasma.

Table 5.3: Voltage coupled to aluminum plate close to generator

<u>condition</u>	<u>a (cm)</u>	<u>V[no plasma]</u>	<u>V[plasma]</u>
RF = 700 W	5	120	70
move plate	2.5	180	100
plate over plasma	1	200	100-300 (fluctuates rapidly)



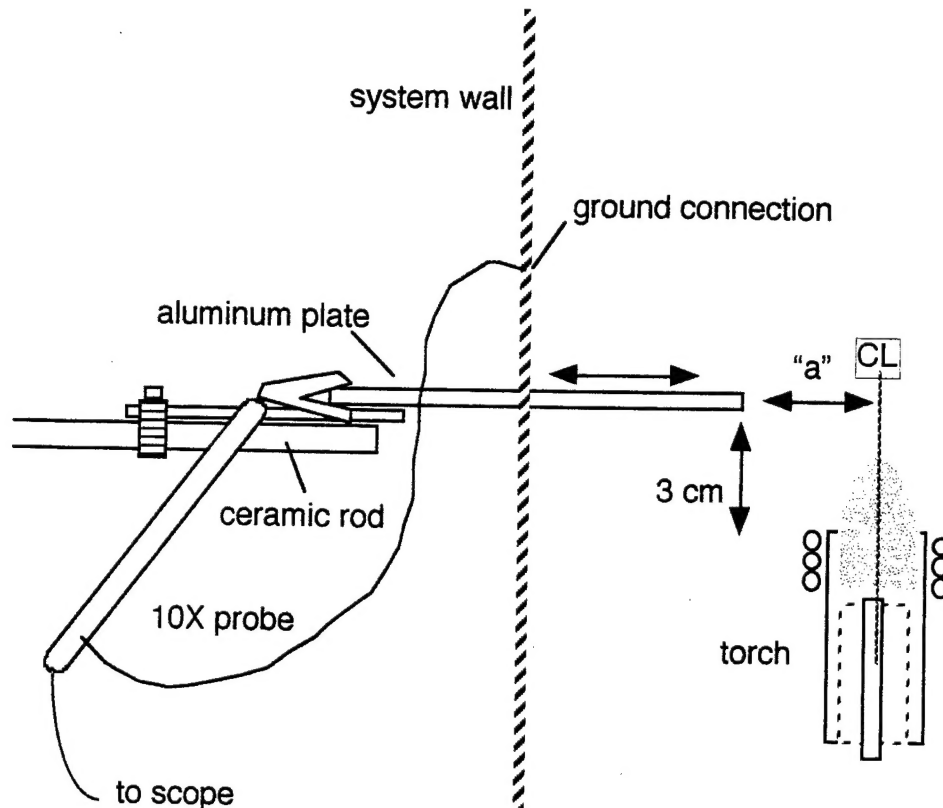


Figure 5.3: Voltage coupling to aluminum plate

## 6] Discussion and Conclusions

We found that no measurable deposition occurs from a wire inserted into the center of an inductive plasma and heated by the ambient: it is not possible to insert the wire into the plasma far enough to induce vaporization without having the supporting wire melt. Inversion of the system (i.e. orienting the torch pointing downwards) will not correct this problem: the molten wire will simply drop through the plasma onto the substrate, with minimal vaporization of the large droplets.

Application of DC bias to a wire in a stable position caused measurable vaporization. We believe this is due to the arcs and consequent transient power delivery to the wire when the grounded substrate comes in electrical contact with the plasma. The deposition rates obtained are several orders of magnitude too small for the envisioned applications, due no doubt to the



very inefficient application of bias power to the wire. (Most of the power is dissipated in the arcs and on the substrate.)

In order to efficiently vaporize a wire, it would be necessary to apply a pulsed bias with pulse times on the order of 10's to 100's of microseconds, and average powers of a few hundred watts. (See discussion in section (3) above.) Such an approach should be able to provide much higher deposition rates, on the order of a few microns per minute, making this approach more applicable to the deposition of thick superelastic films. The increased metal flux will reduce the relative impact of oxidation, but it is still likely to be necessary to enclose the reaction region in an inert gas in order to produce a high quality superelastic film.

In order to implement a biased wire source in practice, it is also necessary to account for and filter the considerable RF potential which is coupled into the plasma from the inductive coil.

We note that a few preliminary experiments using various metal powders were performed. We found that if sufficiently small powder sizes (less than 5 micron diameter) and small gas flows were employed, we could produce smooth adherent films on aluminum substrates with very high deposition rates. Excessive powder diameter or high flow of the carrier gas resulted in films with poor mechanical properties, due presumably to the failure of the particles to vaporize in the plasma if their residence time was too short.

In conclusion, we have shown that a wire inserted into an inductive thermal plasma can be employed as a source of metal vapor for deposition, but that pulsed bias is necessary for acceptable deposition rates. Since such pulse biasing capability was beyond the scope of the current project, we have not been able to deposit NiTi-based films at sufficiently high rates to examine the resulting elastic and metallurgical properties.



## References:

1. A Heat Transfer Textbook (2<sup>nd</sup> ed.), J. Lienhard, Prentice-Hall 1987, appendix A
2. A User's Guide to Vacuum Technology (2<sup>nd</sup> ed.), J. O'Hanlong, Wiley 1989 p. 449

